A Fast Magnetoelectric Device Based on Current-driven Domain Wall Propagation

Meghna G. Mankalale[1], Zhaoxin Liang[1], Angeline Klemm Smith[1], Mahendra DC[2], Mahdi Jamali[1], Jian-Ping Wang[1], and Sachin S. Sapatnekar[1]
[1]*Department of Electrical and Computer Engineering,University of Minnesota, Minneapolis, MN 55455.*
[2]*School of Physics and Astronomy, University of Minnesota, Minneapolis, MN 55455.*
Email: manka018@umn.edu / Phone: (612) 625-0025

Several emerging spintronic devices have recently been proposed, performing computation by (a) generating spin currents based on input magnet states to switch an output magnet state using Spin-Transfer Torque (STT) [1, 2], (b) using multiple nanopillars to drive a domain wall (DW) that switches an output nanopillar using STT [7], and (c) using magnetoelectric (ME) switching at the input, combined with DW automotion, to switch an output state [3]. All of these devices have delays of several nanoseconds. The energy for (a) and (b) is in the range of femtoJoules, while the ME mechanism in (c) facilitates greater energy-efficiency, in the aJ range. These numbers fall some distance away from CMOS, where gate delays and switching energies are in the range of picoseconds (ps) and attoJoules (aJ), respectively.

We propose a new device that uses ME coupling with current-driven DW propagation to ensure energy dissipation in the range of aJ. We leverage recent work that has experimentally demsonstrated faster DW velocities [4, 5]. We explore material parameter values for better delay and energy, and map these to existing/experimental materials.

Our proposed device is shown in Fig. 1(a). It consists of a ferroelectric (*FE*) capacitor at the input and the ouput with a ferromagnetic (*FM*) interconnect in between. A layer of high-resistivity material (*HRM*) is present beneath the *FM*. An oxide layer covers the *FM* between the input and the output capacitors. The different underlying physical mechanisms at the interface or within the structure is shown in Fig. 1(b).

The operation of the device can be understood with the help of the timing diagram in Fig. 2. A voltage, V_{supply}, applied for time $t_{charge,in}$, induces electrical charge on the *FE* capacitor, when $V_{nucleate}$ (transistor T_1) is turned on. This change in the electric polarization of the *FE* capacitor couples with the magnetization of the *FM* beneath it. The resultant effective field from the magnetoelectric coupling nucleates a DW in the *FM* beneath the input *FE* at time $t_{nucleate}$. The DW is then propagated to the output by turning on $V_{propagate}$ (transistor T_2), causing an electric current density, J, to pass through *HRM*, injecting a lateral spin current into the *FM* through Spin-Hall Effect (SHE). The combination of SHE and Dzyaloshinskii-Moriya Interaction (DMI) permits fast DW propagation [4]. Turning on V_{clk} just before the DW reaches the output end introduces electric charge on the output capacitor. The change in the magnetization of FM underneath the output *FE* capacitor induces charge on it by inverse ME coupling. This charge can be transferred to the next logical stage, as in [3].

We model the device operation using the equations in Fig. 3. Using these equations, we can calculate the delay of the device as sum of the time it takes to (a) nucleate a DW ($t_{nucleate}$), (b) propagate the DW ($t_{propagate}$), (c) charge the output *FE* ($t_{charge,out}$), and (d) transfer the charge to next logical stage ($t_{qtransfer}$). The energy consumption of the device is the sum of energy dissipated (a) in the transistor T_2, in *HRM* and (b) while charging the input and output *FE* capacitor. In our implementation, we use the micromagnetics simulator OOMMF [8] to obtain $t_{nucleate}$ and perform the rest of the computation in Matlab. If F is the feature size for a technology, in Fig. 1, we set the dimensions of *FE* to 1F×1F×1nm and *FM* and *HRM* each to 5F×1F×1nm based on analyzing a three-input majority gate layout (Fig. 4). The largest delay occurs when two logic inputs are different from the third, resulting in a single *FE* driving an *FM* interconnect of 5F. The thickness of the *FM* is set to 1nm, enabling the choice of a material with perpendicular magnetic anisotropy. The current density, $J = 9\times10^{10} A/m^2$, is chosen to be below the electromigration limit [12].

Our goal is to perform a design space exploration on material parameters to achieve CMOS-comparable performance, and to use this to guide materials research. For different technology nodes, we show the delay and energy for the three parameter sets in Fig. 5(a), in Fig. 5(b) and (c). The corresponding DW velocities shown in Fig. 5(d) are in agreement with experimentally demonstrated ranges in [4, 5]. Fig. 5(e) shows DW formulation process in OOMMF for parameter Set 1 and Fig. 5(f) lists other simulation parameter values considered. Fig. 5(a) can be mapped to Heusler alloys as M_s and K_u are in the same range as that of MnGa [9]. For *HRM*, we could chose either Pt, β-Ta or β-W. For *FE* capacitor, $BaTiO_3$ is a suitable candidate to couple with the *FM* layer [3]. The damping constant, α can be engineered to be set to 0.05 by adequately doping the *FM*. The choice of the exchange constant, A, is consistent with [11].

In summary, under an appropriate set of parameters, we show that delays of a few hundred ps and energy of about a few hundred aJ are achievable.

[1] B. Behin-Aein *et al.*, Nat. Nanotech., 2010, pp. 266–270.
[2] S. Datta *et al.*, APL, 2012, v.101, 252411.
[3] S.-C. Chang *et al.*, IEEE JxCDC, 2016, v.99.
[4] S. Emori *et al.*, Nat. Mater., 2013, v.12, pp. 611–616.
[5] S.-H. Yang *et al.*, Nat. Nanotech., 2015, v.10, pp. 221–226.
[6] L. Thomas *et al.*, Wiley Online Library, 2007.
[7] D. Nikonov *et al.*, IEEE EDL, 2011, v.32, pp. 1128–1130
[8] M. Donahue *et al.*, OOMMF Users Guide, 1999, NIST.
[9] A. Sugihara *et al.*, APL, 2014, v.104, 132404.
[10] C. L. Zha *et al.*, JAPL, 2011, v.110, 093902.
[11] M. Fiebig, J. Phys. D, 2005, v.38, pp. R123–R152.
[12] S. Kumar *et al.*, Scripta Materialia, 2011, v.65, pp. 277–280

(a)

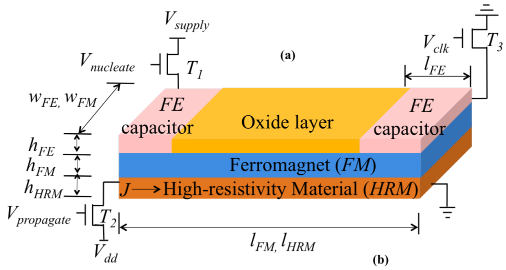

l, w and *h* indicate length, width and height, respectively of the structures denoted by subscript *FE, FM* and *HRM*

(b)

Interface mechanism between structures	
Structure	**DW interconnect**
Input FE capacitor	ME coupling
DW interconnect	STT, SHE, DMI
Output FE capacitor	Inverse ME coupling

Fig. 1: (a) Proposed device and (b) the underlying physical mechanism within and at the interface of the structure.

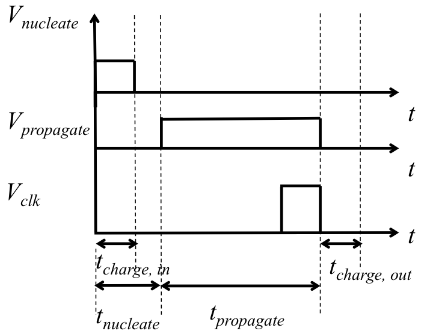

Fig. 2: Timing diagram illustrating the operation of the device.

1. Electric field in *FE*, $\vec{E}_{FE} = \frac{V_{supply}}{h_{FE}}$

2. Electric polarization, $\gamma_v \frac{\partial \vec{P}}{\partial t} = -\frac{\partial \vec{F}_{FE}}{\partial \vec{P}}$ (Landau – Khalatnikov equation)

3. Effective magnetic field, $\vec{H}_{ME} = \alpha_{ME} \frac{h_{int}}{h_{FE}} \vec{P}$

4. Magnetization in *FM*, $\frac{1+\alpha^2}{\gamma} \frac{d\vec{M}}{dt} = -\vec{M} \times \vec{H}_{ME} - \alpha \vec{M} \times (\vec{M} \times \vec{H}_{ME})$ (Landau – Lifshitz – Gilbert equation)

5. Domain wall dynamics, $1 + \alpha^2 \frac{dV_{prop}}{dt} = -\gamma\Delta \frac{H_K}{2} \sin(2\phi) + (1 + \alpha^2\beta) B_{STT} + \gamma\Delta \frac{\pi}{2} [\alpha H_{SHE} + H_{DMI} \sin(\phi)]$

$$1 + \alpha^2 \frac{d\phi}{dt} = -\gamma\alpha \frac{H_K}{2} \sin(2\phi) + \frac{(\beta-\alpha)}{\Delta} B_{STT} + \gamma \frac{\pi}{2} [H_{SHE} \cos(\phi) + \alpha H_{DMI} \sin(\phi)]$$

where $H_{SHE} = \frac{\hbar\, \theta_{SHE} J}{2\mu_0 e M_s h_{FM}}$, $H_{DMI} = \frac{D}{\mu_0 M_s \Delta}$, $B_{STT} = \frac{\mu_B P_{FM} J}{e M_s}$, $\Delta = \frac{\sqrt{A/K_u}}{\sqrt{1+\frac{\mu_0 M_s^2}{K_u}\left[\frac{h_{FM}}{h_{FM}+\Delta} - \frac{h_{FM}}{h_{FM}+w_{FM}}\right] sin^2(\phi)}}$

6. Electric field from Inverse ME, $E_{IME} = \propto_{IME} \frac{h_{int}}{h_{FE}} \vec{M}$

7. Total delay of the device, $t_{delay} = t_{nucleate} + t_{propagate} + t_{charge,out} + t_{qtransfer}$

where, $t_{propagate} = \frac{l_{FM}}{V_{prop}}$

8. Total energy of the device,

$$Energy = C_{FE} V_{supply}^2 + C_{gate,T3} V_{dd}^2 + (J\, w_{HRM} t_{HRM})^2 \left[R_{on,T2} + \frac{\rho_{HRM} l_{HRM}}{w_{HRM} h_{HRM}}\right] t_{propagate}$$

Fig. 3: Governing equations of the device.

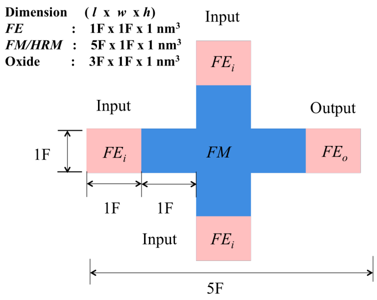

Fig. 4: Layout of a three-input majority gate.

Uniaxial anisotropy constant, K_u = 10^7 erg/cc,
Spin hall angle, θ_{she} = 0.5,
Damping constant, α = 0.05 and
Spin Polarization, P_{FM} = 0.5 for all parameter sets.

- **Energy dominated by the clocking transistors (T_1 & T_2) and the input and output FE capacitors. Comparatively, dissipation in *HRM* and transistor T_2 insignificant.**
- **Delay dominated by the DW propagation.**

Energy-delay tradeoff between parameter sets.

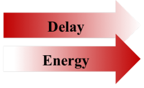

(a)

Set / Parameters	Set 1	Set 2	Set 3
Exchange constant , *A* (μ erg/cm)	**1**	**0.28**	**0.68**
Saturation Magnetization, M_s (emu/cc)	**500**	**300**	**300**
Supply voltage, V_{supply} (V)	**0.93**	**1.50**	**2.12**

(b)

Technology node (1F)	Set 1 (ps)	Set 2 (ps)	Set 3 (ps)
5nm	**128**	**125**	**117**
7nm	**156**	**149**	**124**
10nm	**198**	**184**	**155**

(c)

Technology node (1F)	Set 1 (aJ)	Set 2 (aJ)	Set 3 (aJ)
5nm	**67.4**	**130.6**	**212.0**
7nm	**108.6**	**209.0**	**417.6**
10nm	**173.4**	**375.6**	**701.0**

(d)

Parameter set	DW Velocity (m/s)
Set 1	**362**
Set 2	**420**
Set 3	**540**

(e)

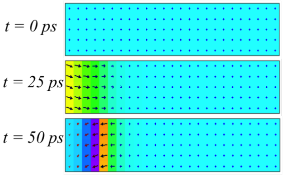

Magnetization into the plane of the magnet at t = 0 (dots). Under the effective magnetic field from the ME coupling, the magnetization starts to rotate (t = 25ps) until a domain wall is formed at t = 50ps

(f)

Parameter	Values
Viscosity coefficient, γ_v	**1.5 x 10^{-2} Vms/C**
Vaccuum permitivitty, ε_0	**8.85 x 10^{-12} F/m**
ME interface thickness, h_{int}	**1 nm**
Speed of light, *c*	**3 x 10^8 m/s**
ME coefficient for input *FE*, α_{ME}	**0.1/c s/m**
ME coefficient for output *FE*, α_{IME}	**0.1/c s/m**
Resistivity of *HRM*, ρ_{HRM}	**10.6 x 10^{-8} Ω-m**
Adiabatic STT paramter, β	**0.4**
DMI constant, |*D*|	**0.5 mJ/m²**
Current density, *J*	**9x10^{10} A/m²**
Bohr magneton, μ_B	**9.274 x 10^{-24} J/T**
V_{dd}	**0.72V**
$R_{on,T2}$	**1000 Ω**
$C_{gate,\ T3}$	**0.1fF**

Fig. 5: (a) Parameter sets considered in this experiment, (b) total delay of the device for different technology nodes for each parameter set, (c) total energy of the device, (d) DW velocities obtained, (e) DW nucleation result from OOMMF for parameter Set 1, and (f) list of parameter values considered in this experiment.